Mechanism Analysis of Rock Breaking Using Static Cracking Agent (SAC)

B.Y. Hao [a] *, S.Y. Hu [a], J. Cheng [b], H. Huang [c], K. Wang [d], L.X. Kang [a]

a College of Mining Engineering, Taiyuan University of Technology, Taiyuan, Shanxi 030024, P.R. China

b State Key Laboratory of Coal Resources and Mine safety, China University of Mining & Technology, Xuzhou Jiangsu 221116, P.R. China

c College of safety Engineering, Chongqing Vocational Institute of Safety & Technology, Chongqing 404000, P.R. China

d College of Mining Engineering, Shanxi Institute of Technology, Yangquan, Shanxi 045000, P.R. China

** Corresponding author: tyuthaoby@126.com*

ABSTRACT

In order to solve the problem of the increase of roadway hanging roof distance in high gas mine working faces close to the goaf side, we used a new rock breaking method, or static cracking method. To clarify, a "static coal and rock cracking agent" was used as the expansion material, and the static cracking was conducted for the roadway roof, under the premise that the anchor cables cannot be demolished. In this way, the hanging roof distance at the rear end of the roadway can be effectively shortened, thereby solving such problems as high upper corner mine gas accumulation, working face air leakage, and roadway support pressure increases.

The static cracking method is currently widely used, despite the fact that there are no scientific experimental data for reference. The SCA has been used under the guidance of a perceptual theory for some time now. In this study, we mainly focus on resolving the crushing law of coal and rock under the action of SCA; analyzing the related factors through establishing a theoretical model; and finally obtaining the crack expansion law and theoretical radius of the expansion, which will provide future guidance for engineering practices.

INTRODUCTION

After the stoping begins and the working face advances, then the rear stoping roadway of the working face becomes a part of the goaf. This results in most of the anchor cable ends on the stoping roadway roof becoming damaged due to the influence of dynamic pressure, and various factors in the service period. The anchor cables cannot be removed, as they still play important roles in the hanging and reinforcing of the roof. Therefore, the roadway roof cannot fall in a timely way with the advancement of the working face, and forms a large range of hanging roof in the rear of the upper and lower ends of the working face. Also, the anchor cables of the open-off cut cannot be removed, resulting in a large top coal caving step distance, preventing the normal coal caving process, and thereby a large amount of top coal is lost. At the same time, large-area caving of the top is also dangerously increased (Wu and Guo, 1999; Qi and Li et al., 2003).

Generally speaking, after the stoping working face has progressed, the anchor rod of the roof and the anchorage of the anchor cable (such as the backing plate, cable head, and clamping piece) in the stoping roadway, will be demolished, causing the roof to lose its support and collapse naturally. This practice proves that the roadway needs to experience a long duration from formation to abandonment. The anchor cable ends will often become damaged, and at this point it is difficult to achieve the ideal anchor removal tool effects. There are still a large number of anchor cables which cannot be demolished, and therefore the implementation effect of the site is very poor.

In order to solve the problem of the increase of the roadway roof hanging distance in a high gas mine working face close to the goaf side, for the purpose of improving coal mining technology and methods, both Chinese and international research teams have conducted studies in terms of various weakening treatment methods. These weakening treatment methods roughly include two categories, hydraulic fracturing (high pressure water injection and static pressure water injection), and pre-splitting blasting (circulating type shallow hole blasting, step distance type deep hole blasting, advanced deep hole pre-splitting blasting, and ground deep hole blasting, etc.). These methods have been applied to the actual sites where hanging roof processing is a problem throughout the world. When compared with the pre-splitting blasting, the cost of the hydraulic fracturing is low and has good safety results. However, the application conditions of this method are harsh, the period is long, the practical effect is not obvious, and therefore the field application is poor. The blasting forced caving method is commonly used in most of the domestic mining areas in order to solve the hanging roof problem. On the other hand, the pre-splitting blasting method is the most effective for processing a roof hanging, as it has advantages such as a short time period, convenient construction, good feasibility, low cost, and good effect. Tt is most common method used in field applications in China and internationally. However, some toxic gases such as CO, SO_2, NO and NO_2 will be generated in the blasting process, and these toxic gases will seriously pollute the environment of the working face. Also, the blasting itself has a certain risk, and therefore the safe production of the working face cannot be guaranteed. The restrictions for a high gas mine in regards to initiating explosive devices are very strict, especially near the goaf, and it is forbidden to use the initiating explosive device to conduct rock breaking. Therefore, it is infeasible to use the pre-splitting blasting method to process the roof hanging problem in high gas mines.

A new method which has introduced is the static cracking method. The “static cracking agent” (SCA) has been used as the expansion material to solve the hanging roof problem at the rear end of the roadway. In this study, we have analyzed the factors which influence the rock breaking processes of the SCA and its rock breaking development law. We then finally obtained the theoretical calculation value of crack expansion radius, through establishing the corresponding mechanical model, thus providing a theoretical basis for the use of this method in the field applications.

ROCK BREAKING MECHANISM OF STATIC CRACKING METHOD

The main principle of the static cracking method is that the solid volume increases after the hydration reaction, in order to cause the cracking agent to produce expansion pressure. After the main component CaO reacts with water, when compared with the solid volume of CaO, the solid volume of the generated Ca $(OH)_2$ is increased by approximately 97.92%. In addition, when the solid volume increases, and the sum of the reaction product's solid volume, along with its molecular internal void volume increment, exceeds the space of the substance system before the reaction. Thereby the results are an increase of the substance volume before and after the reaction which produces expansion pressure (Peng and Huang et al., 1999; He, 2000; Qin and Zhang, 2000; Wang and Zhou et al., 2004; Xu, 2006; Shi and Li et al., 2008; Wang, 2009; Xiao, 2010; Tan, 2012; Xu, 2012; Yang and Liu, 2012).

After the expansion pressure generated by the cracking agent is applied to the wall's single hole, the media hole unit body is subjected to compressive stress in a radial direction, while it is also subjected to the action of tensile stress in the tangential direction. This stress state causes the rocks to break. The stress state is shown below in Fig. 1.

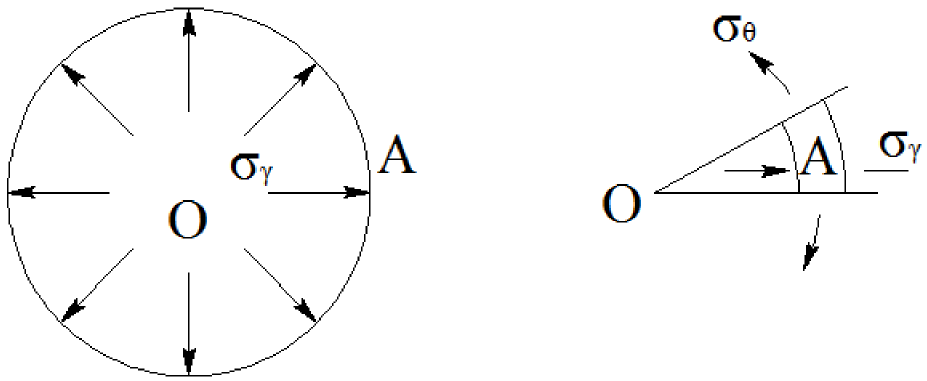

Figure 1: Radial and tangential stress state diagram of the hole unit body

If the expansion pressure σ_γ subjected by Point A is increased, then its subjected tensile stress σ_θ will be also increased. When σ_θ reaches the maximum tensile strength of the object to be broken, the radial cracks will be generated in Point A. With the constant increase of σ_γ, the radial cracks also constantly increases and deepens until the objects become broken.

The question remains of how much expansion pressure is generated by the static cracking agent so that it can crush the materials. The consulted data are shown in the Table 1. The expansion pressure of the cracking agent produced by the existing technology is generally 30 to 80 MPa, while the tensile strength of most rocks is less than 10MPa. Therefore, the static cracking technology can meet the demands of a high gas coal mine when processing its roof.

Table 1: Requirements of rocks with different hardness for static cracking method

Rock types	Compressive strength of rock/MPa	Tensile strength of rock/MPa	Expansion pressure needed by crushing/ MPa
Soft rock	<66	3.6-6.6	8.4-16.8
Medium hard rock	66-120	6.6-10	15.8-26.2
Hard rock	>120	10-13.6	23.6-29.9

SCA CRUSHING THEORY ANALYSIS

Bounded Single Hole Crushing Theory

A bounded single hole model was constructed, as shown in Fig. 2. The expansion pressure generated by any point A on the hole wall in the figure is passed by the surrounding rock mass. When it acts on Point B, whose distance to Point A is L, it is converted into the tensile and compressive stresses subjected by Point B.

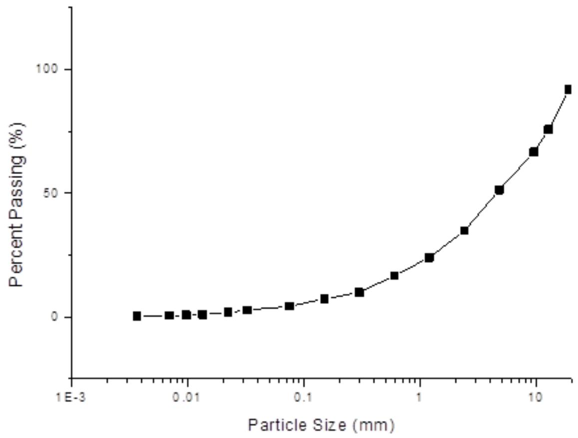

Figure 2: Bounded single hole expansion stress model

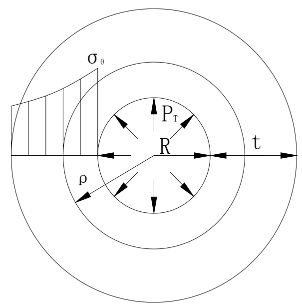

Figure 3: Schematic diagram of bounded single hole expansion stress variation

Under normal circumstances, the compressive strength of the rock is ten times, or even dozens of times that of their tensile strength. The data measured by the laboratory experiments show that the compressive strength of the rock can reach 100.0 to 200.0 MPa. However, their tensile strength is generally between 5.0 MPa and 10.0 MPa, and the maximum does not exceed 10.0 MPa. The expansion pressure generated by the expansion agent used in the research of the bounded hole was above 85 MPa, while the pressure required by the radial fracture of the rock was less than 10.0 MPa, and therefore the expansion agent utilized in this research met the needs of the crushing conditions.

The stress region variations around the expansion agent are as shown in Figure 3. The research shows that, the reaction time of the SCA is generally within 10 hours, and the rock breaking process within this period of time complies with the laws of the elastic mechanics model. The theoretical formula (1) of elastic mechanics model is as follows:

$$\sigma_\theta = \frac{P_r R^2}{(R+t)^2 - R^2}\left[1 + \frac{(R+t)^2}{\rho^2}\right] \tag{1}$$

Where, σ_θ — Tensile stress of Point B, MPa;

P_r — Expansion pressure generated by SCA, MPa;

R — Radius of the hole, mm;

ρ — Distance between any point A on the hole wall and hole heart, mm;

t — Distance between Point B and Point A, mm.

When ρ is very close to the sum of R and t, for instance, when $\rho \to R+t$, then:

$$P_r = \sigma_\theta \left[\frac{t}{R} + \frac{t^2}{2R^2}\right]. \tag{2}$$

When t is very small, for instance, when $t \to 0$ and $\rho \to R$, then:

$$P_r = \sigma_\theta \frac{t}{R} \tag{3}$$

As can be seen from the calculation results of Formulas 2 and 3, when the radius value of the hole R, along with the hole wall radius value t are given, then the value P_r of the expansion pressure generated by the SCA can be calculated.

In Formula 3, when $t \to 0$, then surrounding of the hole can be seen as a thick wall cylinder, and the expansion pressure generated by the SCA is only related to the thickness and radius of the hole wall. At present, the methods of measuring expansion pressure in China and internationally are mainly divided into two types. These are the resistance strain gauge method, and the balance pressure measurement method. In accordance with the determination method of the SCA expansion pressure in China's building material industry standard JC506-2008 *Soundless Cracking Agent*, a Q235 type cold working seamless steel tube, with an inner diameter of 40 mm, a wall thickness of 4 mm, and a length of 500 mm was constructed. One end of this tube was welded, and closed with a 4 mm thick steel plate. A resistance strain gauge, whose resistance value was (120.0 ± 0.2) Ω, and grating specification was 3 mm × 5 mm was then pasted on its surface. A static resistance strain gauge, with a strain measurement range of 0 to 15,000 με, was used to measure the strain value of the gauge, and then the strain value was converted into an expansion pressure using the conversion formula (Jin and Liao, 1989).

In the elastic mechanics theory, the axial, radial, and hoop stress of the outer surface of the thick wall cylinder are as follows:

$$\sigma_z = P_z,\ \sigma_r|_{\rho=R+t} = 0,\ \sigma_\theta|_{\rho=R+t} = \frac{4R^2}{(R+t)(2R+t)}P_r \tag{4}$$

where, P_r is the expansion pressure acting on the radial direction of thick wall cylinder, MPa; P_z is the expansion pressure acting on the axial direction of the thick wall cylinder, MPa; R is the inner diameter of the thick wall cylinder, mm; t is the wall thickness of thick wall cylinder, mm; σ_z is the axial stress of expansion pressure acting on thick wall cylinder, MPa; σ_r is the radial stress of expansion pressure acting on thick wall cylinder, MPa; and σ_θ is the hoop stress of expansion pressure acting on thick wall cylinder, MPa.

The formula of the generalized Hooke's Law is given as follows:

$$\varepsilon_\theta = \frac{1}{E}\left(\sigma_\theta - \nu\sigma_z\right) \tag{5}$$

The, Formula (4) is substituted into Formula (5), and the expansion pressure of the inner side of the thick wall cylinder can be obtained as follows:

$$P_r = E \cdot \frac{\nu\varepsilon_z + \varepsilon_\theta}{1-\nu^2} \cdot \left[\frac{t}{R} + \frac{t^2}{2R^2}\right] \tag{6}$$

where, E is the elastic modulus of thick wall cylinder, MPa; ν is Poisson's ratio of thick wall cylinder; ε_z is the axial strain value; and ε_θ is the hoop strain value.

Crushing Theory of Single Hole with Many Free Surfaces

When the object to be broken has many free surfaces, the main factor affecting the crack generation is shear stress, as shown in Fig. 4. Under the action of shear stress, the cracks are first generated from the hole wall at the bottom of the hole, and then they begin to slowly spread outward along the bottom edge until they expand to the free surfaces.

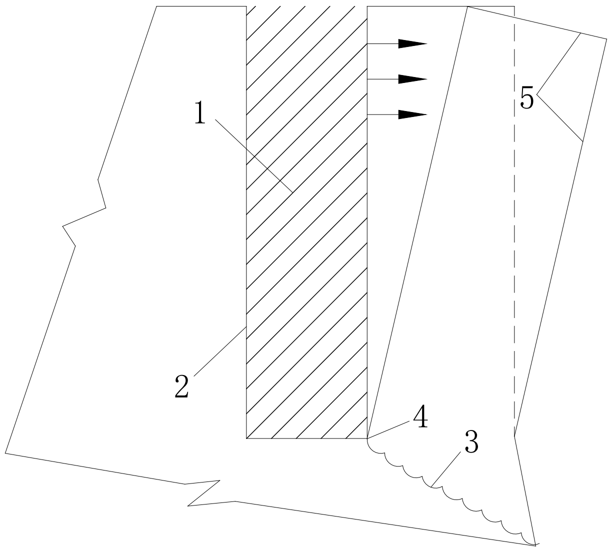

1. Static cracking agent; 2. Filling hole; 3. Micro crack; 4. Fracture stress; 5. Free surface

Figure 4: Schematic diagram of the crack generation of the material to be broken with many free surfaces

Multi-hole Crushing Theory

During multi-hole crushing, the crack generation is not only related to the expansion pressure of the SCA itself, along with the rock crushing strength, but it is also affected by the interaction between the holes. Two charge holes which are close to each other jointly crushing rocks, are illustrated in Figure 5's mechanical model, where O_1 and O_2 represent Hole 1 and Hole 2, respectively.

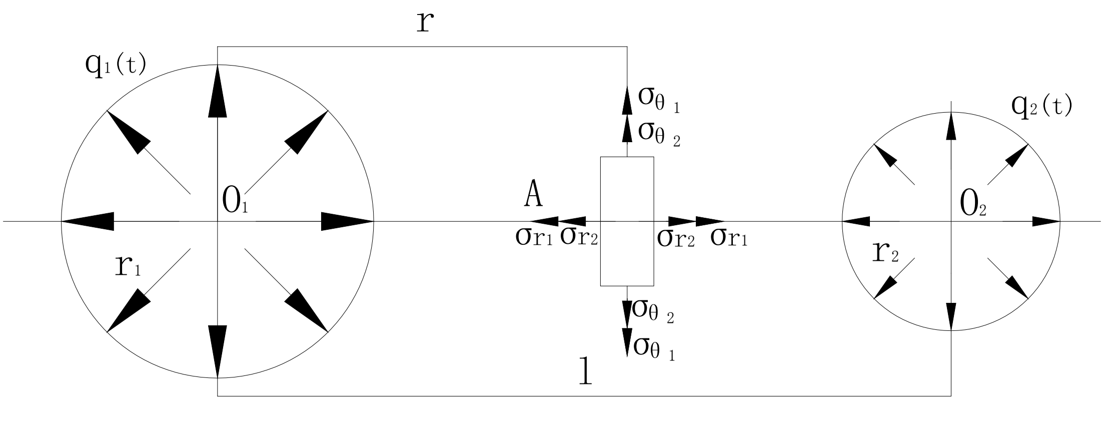

Figure 5: Force diagram of rock breaking model with two holes

During the actual application of engineering, when comparing the dimension of the object to be broken, the construction hole diameter is very small, and therefore it can be deemed that the charge hole is in an infinite medium. The SCA expansion process is a relatively slow process, and it changes little within a short time period. Therefore, the SCA expansion process can be seen as static. In view of the two above-mentioned reasons, the crushing effect of the model can be seen as a simple superposition of the action of the two holes. The superposition force formula of the two holes is as follows:

$$\begin{cases} \sigma_r = \sigma_{r1} + \sigma_{r2} = -\left[\frac{r_1^2}{r^2} q_1(t) + \frac{r_2^2}{(1-r)^2} q_2(t) \right] \\ \sigma_\theta = \sigma_{\theta 1} + \sigma_{\theta 2} = \frac{r_1^2}{r^2} q_1(t) + \frac{r_2^2}{(1-r)^2} q_2(t) \end{cases} \tag{7}$$

Then:

$$\sigma = \left| \sigma_r - \sigma_\theta \right| = \frac{2r_1^2}{r^2} q_1(t) + \frac{2r_2^2}{(1-r)^2} q_2(t) \tag{8}$$

The reciprocal of the above formula *r* is as follows:

$$\sigma' \Big|_r = -\frac{4r_1^2}{r^3} q_1(t) - \frac{4r_2^2}{(l-r)^3} q_2(t) \tag{9}$$

When, $\sigma' \Big|_r = 0$,

$$r = \frac{1}{\left[1 + \sqrt[3]{\frac{r_2^2 q_2(t)}{r_1^2 q_1(t)}} \right]} \tag{10}$$

In Formula 10, *r* is the extreme value of the point, and its stress is as follows:

$$\sigma = \frac{2r_1^2 q_1(t)}{l^2} \left[1 + \sqrt[3]{\frac{r_2^2 q_2(t)}{r_1^2 q_1(t)}} \right]^2 + \frac{2r_2^2 q_2(t)}{\sqrt[3]{\frac{r_2^2 q_2(t)}{r_1^2 q_1(t)}}^2} \left[1 + \sqrt[3]{\frac{r_2^2 q_2(t)}{r_1^2 q_1(t)}} \right]^2 \tag{11}$$

When the left critical value $r = r_1$,

$$\sigma_{左} = 2q_1(t) + \frac{2r_2^2}{(l-r_1)^2} q_2(t) \tag{12}$$

When the right critical value $r = r_2$,

$$\sigma_{右} = \frac{2r_1^2}{(l-r_2)^2} q_1(t) + 2q_2(t) \tag{13}$$

While the minimum stress occurs in the connection line of O1 and O2, and thereby we can obtain:

$$\sigma_{\min} = \min\{\sigma, \sigma_{左}, \sigma_{右}\} \tag{14}$$

In most cases, the dimensions of the construction holes are same. That is to say, $r = r_1 = r_2$, $q = q_1 = q_2$, then:

$$\sigma_{\min} = \min\left\{\frac{8r^2 q}{(1+2r)^2}, 2q + \frac{2r^2}{(1-r)^2}, 2q + \frac{2r^2 q}{(1-r)^2}\right\} = \frac{8rq}{(1+2r)^2} \tag{15}$$

From the third strength theory, we can determine that the condition to meet crushing is as follows:

$$\sigma_{\min} \geq [\sigma] \tag{16}$$

Where, $[\sigma]$ is the ultimate tensile strength of the object to be broken, then:

$$\frac{8rq}{(1+2r)^2} \geq [\sigma] \tag{17}$$

Therefore we can obtain:

$$q \geq \frac{(1+2r)^2}{8r^2}[\sigma] \tag{18}$$

From Formula 11 we can calculate that the size of σ is related to the hole diameter r, and the hole distance l. The hole diameter r should be increased as much as possible, while the hole distance l should be reduced, in order to make σ greater.

MECHANICAL ANALYSIS OF HOLE FISSURE DEVELOPMENT

During the 1980s, Dr. Jin Zongzhe mentioned the three stages of brittle material failure, which are the micro crack stage, transmission stage, and splitting stage, in his published article “Splitting Mechanism of Rock and Concrete under Action of Expansion Pressure” (2008).

In regards to the micro crack stage, Dr. Jin Zongzhe believed that micro cracks existed in the interior of brittle materials, and the SCA expansion pressure made the cracks in the defects increase or expand. Then, tiny plastic deformations occurred. Initially the stress subjected by the brittle materials was linear in the micro crack stage, due to the fact that the tiny plastic deformations occurred in the crushing occurrence zone (damage zone), and the stress then became nonlinear.

For the transmission stage, after the occurrence of micro crack stage, a portion of the stress is released to the surrounding rock mass through the tiny cracks. There is also a part of the stress which makes the tiny cracks generate plastic deformations, and in this way reduces the expansion resistance. However, with the continuance of the SCA hydration reaction, the amount of SCA is constantly increased, and the generated expansion pressure is also constantly increased. With the crushing occurrence zone as the medium, the expansion pressure spreads outside the zone, forcing the existing crack expansion to become larger and wider, and new cracks are generated in the transmission process of the expansion pressure.

In regards to the splitting stage, after the transmission stage, the expansion pressure is transmitted to the free surfaces of the object to be broken, and the energy is gathered there. At the same time, the cracks also expand to the free surfaces, and therefore the splitting phenomenon appears in the free surfaces. As the hydration reaction of the SCA occurs, the energy gathered in the free surfaces increases, and when the energy reaches the upper limit of the energy which the free surfaces can bear, then the gathered energy is suddenly released, the object to be broken is split, and the crushing process is completed.

As described in Section 3.3, compared with the dimension of the object to be broken, the construction hole diameter is very small, and therefore it can be concluded that the construction hole is in an infinite medium. The stress field subjected by it is as follows:

$$\begin{cases} \sigma_r = -\dfrac{R^2}{r^2} q(t) \\ \sigma_\theta = \dfrac{R^2}{r^2} q(t) \end{cases} \tag{19}$$

where σ_r is the radial stress, MPa; σ_θ represents the hoop stress, MPa; $q(t)$ is the expansion pressure load changing with time, kN; R represents the hole radius, mm; and r is the distance between any point and hole center point, mm.

When, $r = R$, $\sigma_r = -q(t)$ and $\sigma_\theta = q(t)$, the maximum principal stress appears in the hole wall, and its value is $q(t)$. By assuming that there are N holes in the single row, as shown in Fig. 6, according to the stress field superposition principle, the tensile stress on the axle centre surface of the holes A_i and A_{i+1} is as follows:

$$\sigma_\theta = \frac{R^2}{r^2} q(t) + \sum_{n-1}^{i-1} \frac{R^2}{(nW+r)^2} q(t) + \sum_{n-1}^{N-i} \frac{R^2}{(nW-r)^2} q(t) \quad (R \le r \le W - R) \tag{20}$$

where W is the blast hole spacing; and N represents the number of blast holes in a single row.

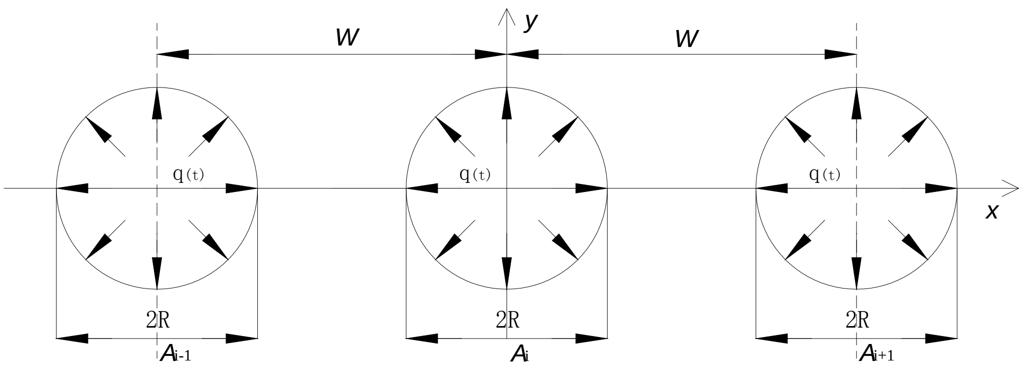

Figure 6: Single row multi-hole force model

Formula 20 is suitable for the holes without a stress concentration. Due to the combined action of A_{i-1} and A_{i+1} on A_i, the stress concentration phenomenon will be generated in the hole A_i, and if the stress concentration coefficient in the place is set as K, then the tensile stress subjected by A_i is as follows:

$$\sigma_{\theta\max} = q(t) + \sum_{n-1}^{i-1} \frac{KR^2}{(nW+R)^2} q(t) + \sum_{n-1}^{N-i} \frac{KR^2}{(nW-R)^2} q(t) \quad (r = R) \qquad (21)$$

Since R is much smaller than W, the items with R in the denominator will be omitted, and then Formula 21 can be simplified as:

$$\sigma'_{\theta\max} = q(t) + \frac{KR^2}{W^2}\left(\sum_{n-1}^{i-1}\frac{1}{n^2} + \sum_{n-1}^{N-i}\frac{1}{n^2}\right) q(t) \qquad (22)$$

The above formula represents the expansion tensile stress during the charge of a single row hole. It is known that, when compared with a single hole maximum tensile stress, a multi-hole maximum tensile stress is increased by M; where, M is as follows:

$$M = \frac{KR^2}{W^2}\left(\sum_{n-1}^{i-1}\frac{1}{n^2} + \sum_{n-1}^{N-i}\frac{1}{n^2}\right) q(t) \qquad (23)$$

Formula 23 represents the tensile stress subjected by A_i during a multi-hole charge. There is a very critical variable in the tensile stress, which is namely the stress concentration coefficient K. The question remains of where does K take its value. Based on the single hole stress condition model shown in Fig. 7, we will analyze the conditions for the values of K.

In the initial state, the stress strength factor of the model is as follows:

$$K_1 = Fq(t)\sqrt{\pi(a+R)} \qquad (24)$$

Where a represents the single edge crack length, mm; and F is the influence coefficient.

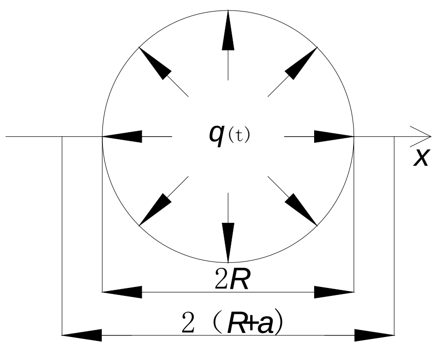

Figure 7: Single hole fracture model

As the reaction is conducted, the force state of a single hole fracture model is seen as the uniform load acting on the cracking surface, and the force analysis conducted for it is as shown in Fig. 8.

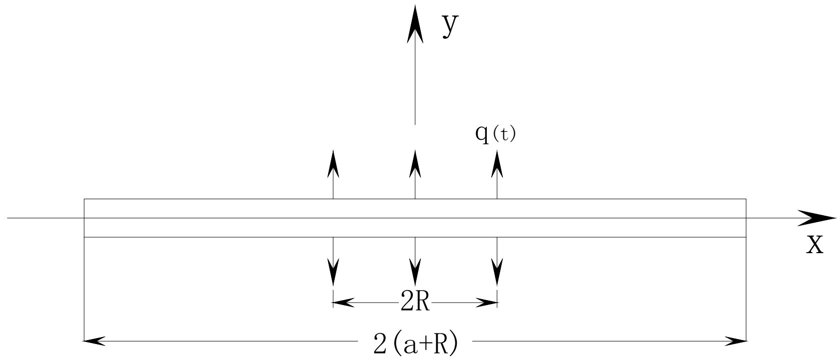

Figure 8: Uniform load acting on single hole fracture model

In this state, the strength factor is as follows:

$$K_2 = \frac{2q(t)}{\pi}\sqrt{\pi(a+R)}\cdot\sin^{-1}(-\frac{R}{a+R}) \quad (25)$$

The cracks continue to expand, and during the later period, the force state of the model can be further simplified into the mechanical model of a concentrated force action as shown in Fig. 9.

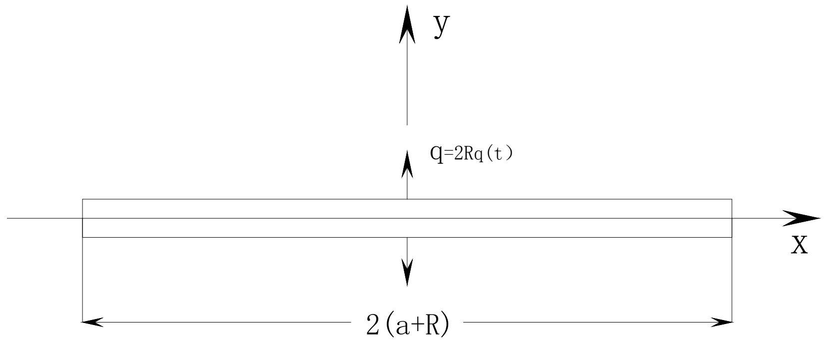

Figure 9: Concentrated force acting on single hole fracture model

The strength factor of the mechanical model of a concentrated force action is as follows:

$$K_3 = \frac{2q(t)}{\sqrt{\pi(a+R)}} \quad (26)$$

When, R = 20 mm, the changes of K_1, K_2 and K_3 are shown in Fig. 10; when $a \geq 2R$, and the error is within 5%, then the action subjected by the crack surfaces in Formulas 24, 25 and 26 can become uniform loads, and the strength factor at this time is as follows:

$$K = \frac{2\sqrt{2}Rq(t)}{\sqrt{W\sin\frac{2\pi(a+R)}{W}}} \quad (27)$$

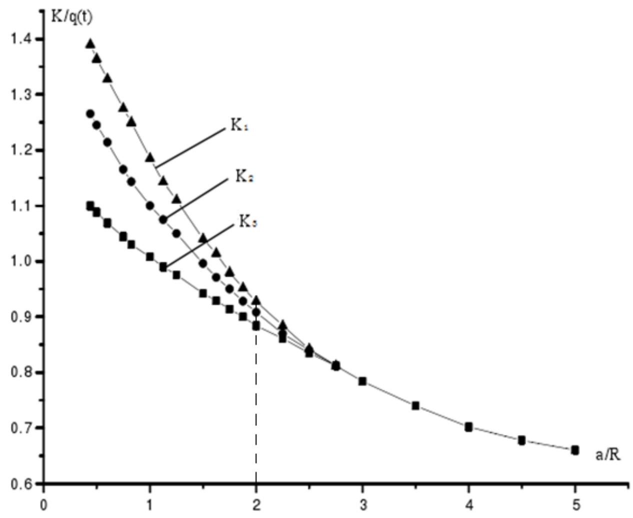

Figure 10: $K/q(t)-a/R$ curve at R =20mm

As the hydration reaction of the SCA is conducted, the expansion pressure is constantly increased, and the expansion speed of the cracks is also constantly increased. When, K=K_c, under the condition of $a \geq 2R$, then the crack expansion meets the following:

$$K_c = \frac{2q(t)}{\pi}\sqrt{w\tan\frac{\pi(a+R)}{W}}\sin^{-1}\frac{\sin\frac{\pi R}{W}}{\sin\frac{\pi(a+R)}{W}} \tag{28}$$

When R=200mm and $W = 400$mm, then the SCA expansion pressure is calculated according to Formula 6, and the crack length is calculated according to Formula 28. When

$$a + R \leq \frac{W}{4}$$

then the cracks are constantly increased, and the expansion pressure needed by the rock breaking is also increased constantly.

The expansion pressure generated by the quantitative SCA is also limited, and also the crack range can only develop to a certain distance. Therefore, the expansion pressure must be increased in order to make the crack expansion distance increase.

CRACK GENERATION FORM

Single Hole Crack Generation Form

When the object to be broken is square, the crack formation which is formed by using a single hole charge crushing square material is shown as shown in Fig. 11. First of all, the first cracks A and C are generated along the minimum resistance line direction. Then, the fracture surface is formed. At this point, the energy within the hole is not released completely; the expansion pressure continues to be generated; the second cracks B or D are formed on the direction which is perpendicular to A; and sometimes the cracks B and D do not appear simultaneously.

When the object to be broken is square, then the actual single hole crack generation form observed in the laboratory experiments is a shown in Fig. 12.

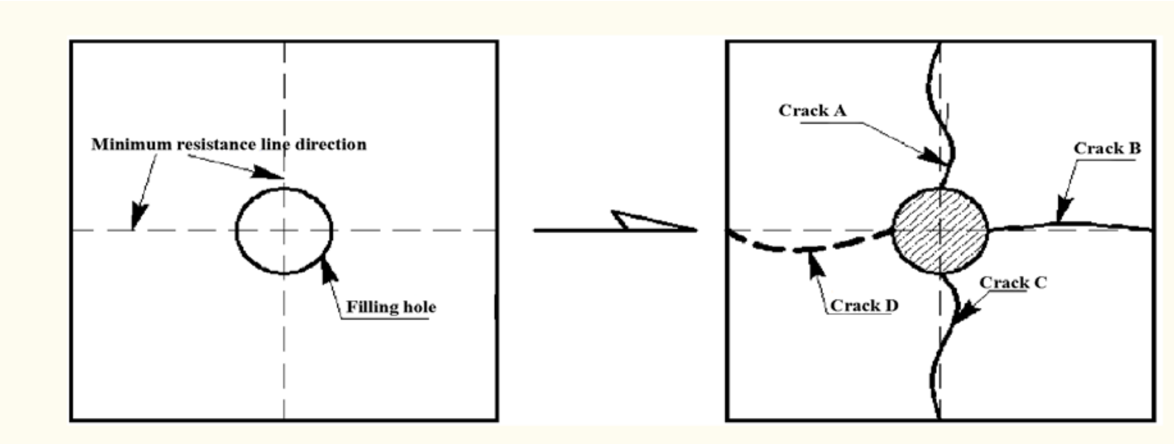

Figure 11: Schematic diagram of single hole crack generation form (square broken material)

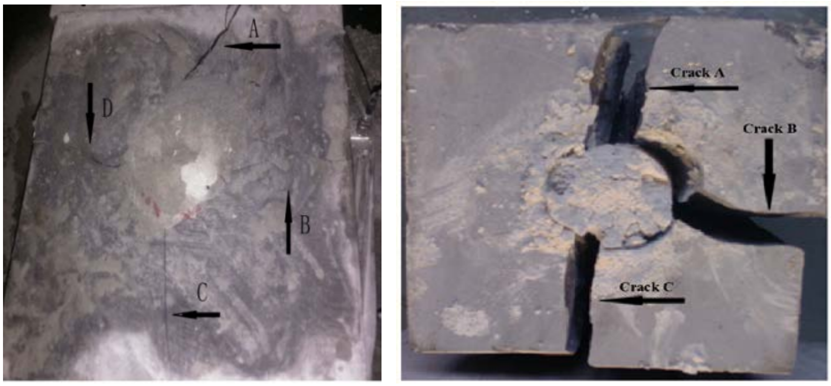

Figure 12: Single hole crack expansion in square broken material

When the object to be broken is round, then two kinds of crack development forms will appear in the cracks formed by using a single hole charge crushing round material, which are a linear type, and a divergent type, as shown in Fig. 13. The crack development observed in the laboratory experiments is shown in Fig. 14.

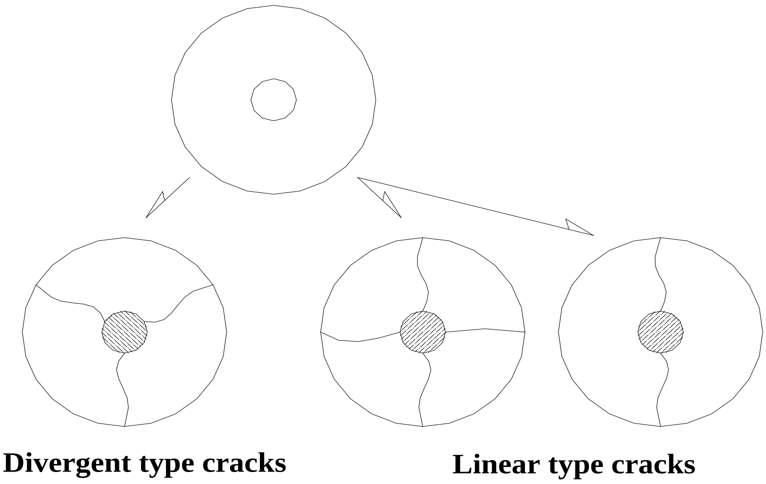

Figure 13: Schematic diagram of a single hole crack generation form (round broken material)

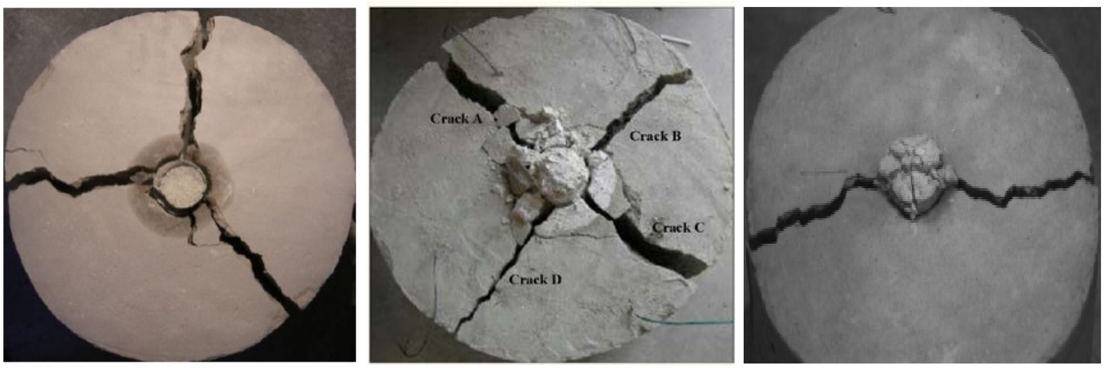

Figure 14: Single hole crack expansion in round broken material

Multi-hole Crack Generation Form

Double hole crack expansion

During a double hole charge, the expansion pressure generated by the reagents within the two holes interacts. First of all, the main crack appears along the minimum resistance line direction (namely, the connection line of the two holes), with the progress of the expansion process. The main crack passes through the two charge holes, and expands to the edges of the object to be broken. In this case, the crack expansion trend is as shown in Fig. 15, and it has been verified in laboratory experiments, as shown in Fig. 16.

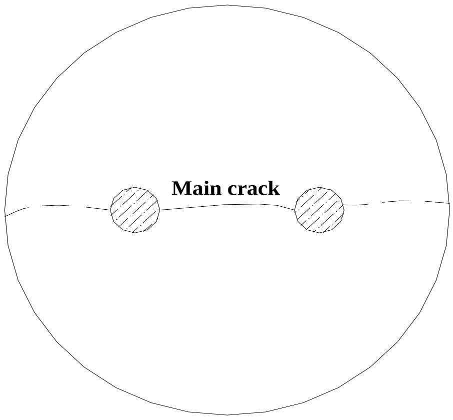

Figure 15: Schematic diagram of double hole crack expansion trend

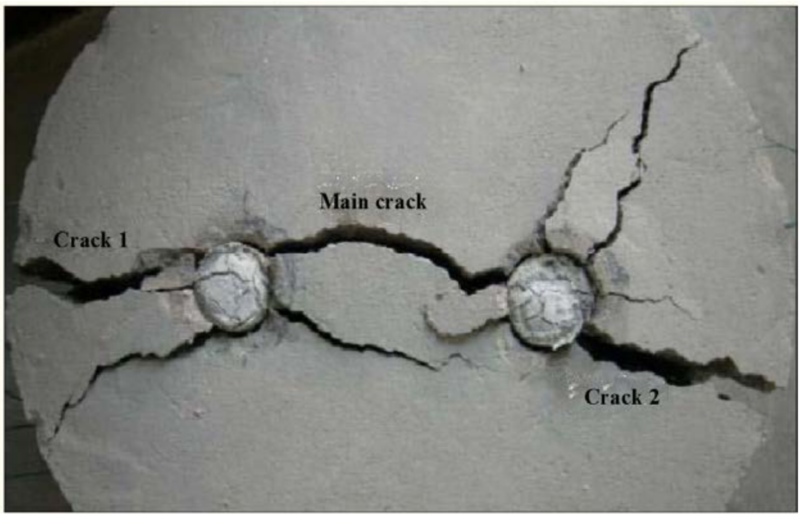

Figure 16: Actual situation of double hole crack development in lab (Du, 2008)

Multi-hole crack expansion

When there are many holes of close proximity inside the object to be broken, then the cracks generated by the adjacent charge holes will connect with each other, forming the expansion form shown in Fig. 17. The situation obtained in the laboratory is as shown in Fig. 18. The cracks do not appear between top hole and center hole in Fig. 18, mainly due to the object to be broken being inhomogeneous (Qin and Men et al., 2009).

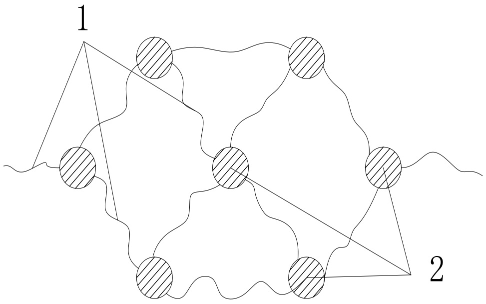

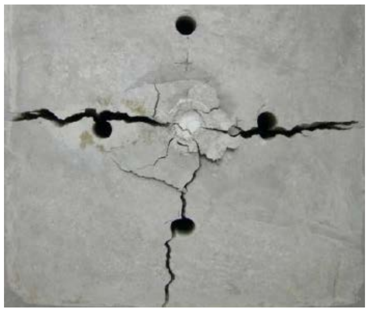

Figure 17: Schematic diagram of multi-hole crack expansion trend; Fig. 18 Actual situation of multi-hole crack development in lab (Du, 2008)

CRACK EXPANSION ANALYSIS

Expansion Model

Using a combination of the contents of the above theories and analysis results, the crack expansion model shown in Fig. 19 was established (Li and Gu et al., 2009; Li and He et al., 2010).

When the crack length a is very small, the borehole can also be seen as a part of the crack, and assuming that the entire model is in an infinite medium, then the distribution stress perpendicular to the crack surface and subjected by the model is $q(t)$, and its stress strength factor is as follows:

$$K_I^* = 2\sqrt{\frac{a}{\pi}} q(t) \arcsin(\frac{d}{a}) \tag{29}$$

where, K_I^* is the crack tip stress strength factor, $N / mm^{\frac{3}{2}}$; d is the borehole diameter, mm; and a represents the crack length, mm.

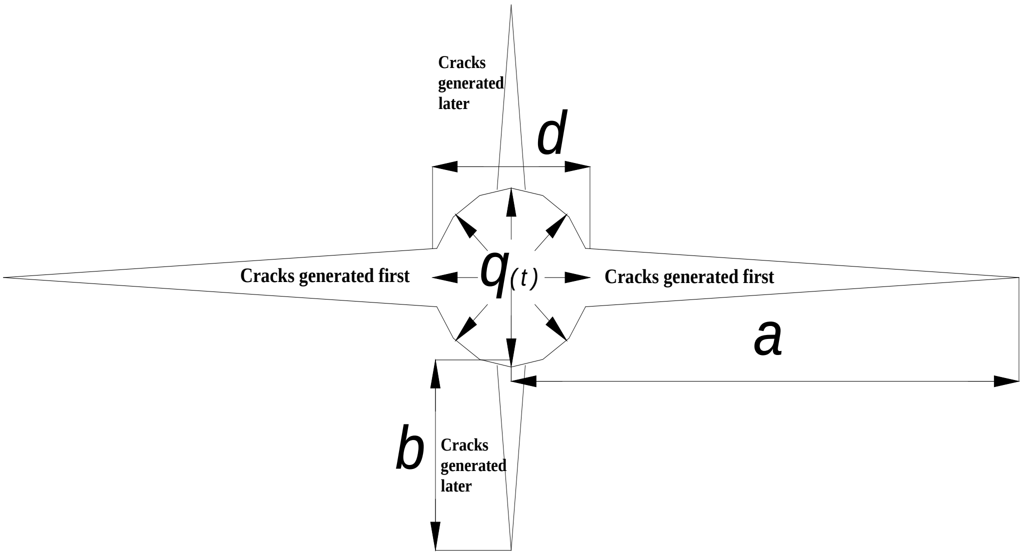

Figure 19: Crack expansion model

When a is much larger than d, then the model can be seen as the cracks of a pair of concentrated stress P acting on the upper and lower surfaces of the center. $P = \lim_{r \to 0} 2q(t)d$, where, r is the distance between any point and the hole center. Then, the crack stress factor can also be expressed as:

$$K^*_{先} = \frac{P}{\sqrt{\pi a}} \tag{30}$$

先：First

$$K^*_{后} = \frac{P}{\sqrt{\pi b}} \tag{31}$$

后：Later

Theoretical Calculation of Crack Expansion Radius

In the hydration process of the static cracking agent, its volume expands; the expansion pressure applied to the hole also continues to increase; and the crack tip stress strength factor around the borehole rises accordingly. However, when the strength factor reaches the rock fracture toughness, the cracks begin to expand outward. In Formulas 30 and 31, when P is unchanged, the smaller the crack length a is found to be, and the greater the stress strength factor becomes. When $K^*_{主}$ or $K^*_{次}$ reaches the rock fracture toughness K_{IC}, then the cracks begin to expand, the crack length increases, and the stress strength factor decreases rapidly. When less than the rock fracture toughness K_{IC}, crack arrest appears. Also, when P increases constantly, the expansion and crack arrest processes of the above-mentioned cracks occur constantly.

The fracture toughness K_{IC} of the corresponding rock can be obtained through the measured uniaxial compressive strength σ_c of the rock as follows:

$$K_{IC}=0.0265\sigma_c+0.0014 . \tag{32}$$

Under normal circumstances, $a<b$, and therefore $K^*_{先}<K^*_{后}$. According to the crack expansion minimum crack arrest equation:

$$K^*_{先}=K_{IC} \tag{33}$$

Formulas 30 and 32 are substituted into Formula 33, and then the following formula can be obtained:

$$a=\frac{q^2(t)}{\pi(0.0256\sigma_c+0.0014)^2} \tag{34}$$

Formula 34 is the theoretical radius of the crack expansion. It can be seen form the formula that, when the static cracking method is used to process the hanging roof problem, the reasonable spacing of the borehole was found to be $2a$.

SUMMARY

(1) We provided the calculation formula of the expansion pressure of the cracking agent by analyzing the bounded single hole crushing theory; the crushing theory of single hole with many free surfaces; and the multi-hole crushing theory. According to the Formula

$$q\geq\frac{(1+2r)^2}{8r^2}[\sigma]$$

we can know that, the size of σ is related to the hole diameter r and the hole distance l. The hole diameter r should be increased as much as possible, while the hole distance l should be reduced, in order to increase σ.

(2) For a single crushing hole, when the SCA is used to crush square materials, the generated cracks are mainly exhibited as a linear type. When the SCA is used to crush round materials, the generated cracks are mainly exhibited as both linear and divergent types. Also, when there are many crushing holes, the cracks generated by the adjacent charge holes connect with each other.

(3) In regards to the established “cross” crossover crack expansion model, the occurrence time of the cracks generated first and the cracks generated later were not synchronized. The theoretical radius of the crack expansion is as follows:

$$a = \frac{q^2(t)}{\pi(0.0256\sigma_c + 0.0014)^2}.$$

Therefore, when the static cracking method is used to process a hanging roof problem, the reasonable spacing of the borehole was found to be $2a$.

ACKNOWLEDGEMENTS

Supported jointly by the Key Technology R&D Program of Shanxi Province, China,(Grant No.20121101009-03) and the Natural Science Fund of Shanxi Province, China, (Grant No.2014011044-1).

REFERENCES

1. (2008). Building Materials Industry Standard of the People' s Republic of China. JC506-2008. Beijing, China Standard Press.
2. Du, L. (2008). Test Study on Rock Breaking Mechanism of Static Cracking Agent. Beijing, China University of Mining and Technology.
3. He, T. (2000). "Prediction of Breaking Position of Working Face Hanging Roof in Roadway along Gob." Journal of China Coal Society **25** (1): 28-31.
4. Jin, Z. and H. Liao (1989). "Splitting Mechanism of Rock and Concrete under Action of Expansion Pressure." Journal of Rock Mechanics and Engineering **18** (1): 19-26.
5. Li, J. and D. Gu, (2009). "Relevant Law of Rock Fracture Toughness and Compressive Strength." Journal of Central South University (Natural Science Edition) **40** (6): 1695-1699.
6. Li, S. and T. He, (2010). Introduction of Rock Fracture Mechanics. Beijing, Press of University of Science and Technology of China.
7. Peng, J. and Z. Huang, (1999). "Static Cracking Demolition of Reinforced Concrete Arch Bridge." Journal of Shijiazhuang Railway Institute **12** (1): 44-47.
8. Qi, M. and H. Li, (2003). "State Analysis of Stoping Roadway Before and After Demolition of Anchor Cable and Rigging Demolition Technology." Coal Engineering(6): 45-47.
9. Qin, B. and Y. Men, (2009). "Test Study on Expansion Characteristics and Mechanical Characteristics of Limestone Under High Temperature." Journal of Disaster Prevention and Mitigation Engineering **29** (6): 702-707.
10. Qin, L. and L. Zhang (2000). "Study on Roof Structure and Stability of Fully Mechanized Caving Face End." Coal Mine Modernization(6): 14-16.
11. Shi, H. and J. Li, (2008). "Practice of Static Cracking Agent in Downhole Wall-caving [J]. , 2008, (11)." Express Information of Mining Industry(11): 93-95.

12. Tan, Y. (2012). Application and Research of Static Cracking Agent in Stoping Working Face End Hanging Roof Processing. Taiyuan, Taiyuan University of Technology.

13. Wang, J. and J. Zhou, (2004). "Application of Static Cracking Method in Coal Mine Equipment Foundation Demolition." Blasting **21** (3): 65-66.

14. Wang, Y. (2009). Study on Static Fracture Technology and Mechanism. Wuhan, Wuhan University of Technology.

15. Wu, X. and H. Guo (1999). "Prediction and Prevention of Hard Roof Rock Burst." (3): 211-214.

16. Xiao, Y. (2010). "Study on Structural Stability of Fully Mechanized Caving Face End Zone." **19** (2): 83-88, 103.

17. Xu, D. (2012). "Development and Application of Static Cracking Technology." Modern Mining(5): 105-106, 109.

18. Xu, Y. (2006). Mining Science. Xuzhou, China University of Mining and Technology Press.

19. Yang, P. and C. Liu (2012). "Basic Top Structure and Reasonable Support Parameters of Fully Mechanized Caving Face End." Journal of Mining and Safety Engineering **29** (1): 26-32.